Supplementary Material for "Cross-Evaluation of Stiffness Measurement Methods for Hydrogels"

Nathan R. Richbourg,[1] Manuel K. Rausch,[1,2,3] Nicholas A. Peppas[1,4-6]*

[1]Department of Biomedical Engineering, University of Texas, Austin, TX 78712, USA.

[2]Department of Aerospace Engineering & Engineering Mechanics, University of Texas, Austin, TX 78712, USA.

[3]Oden Institute for Computational Engineering & Sciences, University of Texas, Austin, TX 78712, USA.

[4]McKetta Department of Chemical Engineering, University of Texas, Austin, TX 78712, USA.

[5]Division of Molecular Therapeutics and Drug Delivery, College of Pharmacy, University of Texas, Austin, TX 78712, USA.

[6]Departments of Surgery and Pediatrics, Dell Medical School, University of Texas, Austin, TX 78712, USA.

*Corresponding Author Contact: peppas@che.utexas.edu

Custom dog-bone sample cutter and shoulder-supporting clamps for tensile testing:

Our design for a matching sample dog-bone cutter and shoulder-supporting clamps was initially based upon the work of Moy et al.[49] However, their design required that each shoulder included a large volume of the sample for a relatively small gauge area. For our samples and characterization goals, their system was not appropriate, so we designed a dog-bone shape with much smaller shoulders. Because our samples were already synthesized as flat films and because the hydrogels tended to stick to molds after synthesis, we designed and produced the dog-bone shape as a steel die-cutter. The STL file, designed using Fusion 360 (Autodesk, Inc., San Rafael, CA), for the die-cutter is available at the STL Files link below. The file was custom-milled into a steel die by our campus machine shop. Shoulder holder pieces were made to complement the steel-cut dogbone samples and grip the sample, also designed using Fusion 360 software. The shoulder holder STL file that was used for this study is available at the STL file link below. Another version of the shoulder holder was developed later to address slipping issues associated with the first shoulder holder design, but it has not been tested yet. STL file is available at the STL file link below. All shoulder holders were made using a Form 2 3D printer (Formlabs, Somerville, MA).

Links for R scripts, protocols, and data:

All publicly available files associated with the manuscript:

https://doi.org/10.6084/m9.figshare.c.5915942.v2

R Scripts: https://doi.org/10.6084/m9.figshare.19424237.v1

Protocols: https://doi.org/10.6084/m9.figshare.19424252.v1

Summary Data: https://doi.org/10.6084/m9.figshare.19424255.v1

STL Files: https://doi.org/10.6084/m9.figshare.19424258.v1

Raw Tension Data: https://doi.org/10.6084/m9.figshare.20343786.v1

Raw Compression Data: https://doi.org/10.6084/m9.figshare.20343684.v1

Processed Compression Data: https://doi.org/10.6084/m9.figshare.20343678.v1

Raw Rheology Data: https://doi.org/10.6084/m9.figshare.20343777.v1

Raw Macroindentation Data: https://doi.org/10.6084/m9.figshare.20343723.v1

Processed Macroindentation Data: https://doi.org/10.6084/m9.figshare.20343696.v1

Raw Nanoindentation Data: https://doi.org/10.6084/m9.figshare.20343729.v1

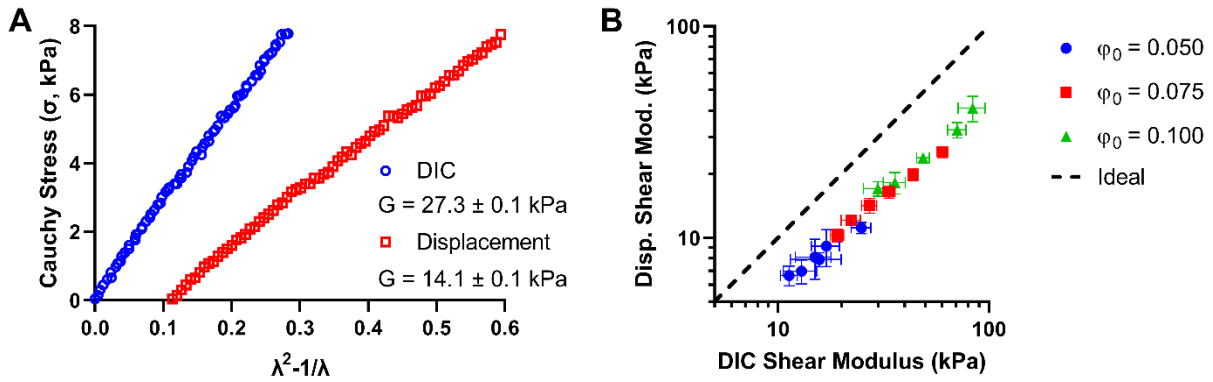

Supplementary Figure S1. DIC-based shear modulus and displacement-based shear modulus in an example tensile testing experiment (A) and for all formulations (B). Shear moduli were calculated from the slope of the best fit lines for each experiment. DIC-based shear moduli were used in final data analyses because they represent local strain within the gauge area of the sample. The example data was taken from the first tensile test sample for the $\varphi_0 = 0.075, N_j = 50$ formulation (Tensile Exp. ID S1-PVA-M-75-100-1). The trend of DIC-based shear moduli being twice that of displacement-based shear moduli is conserved across all formulations.

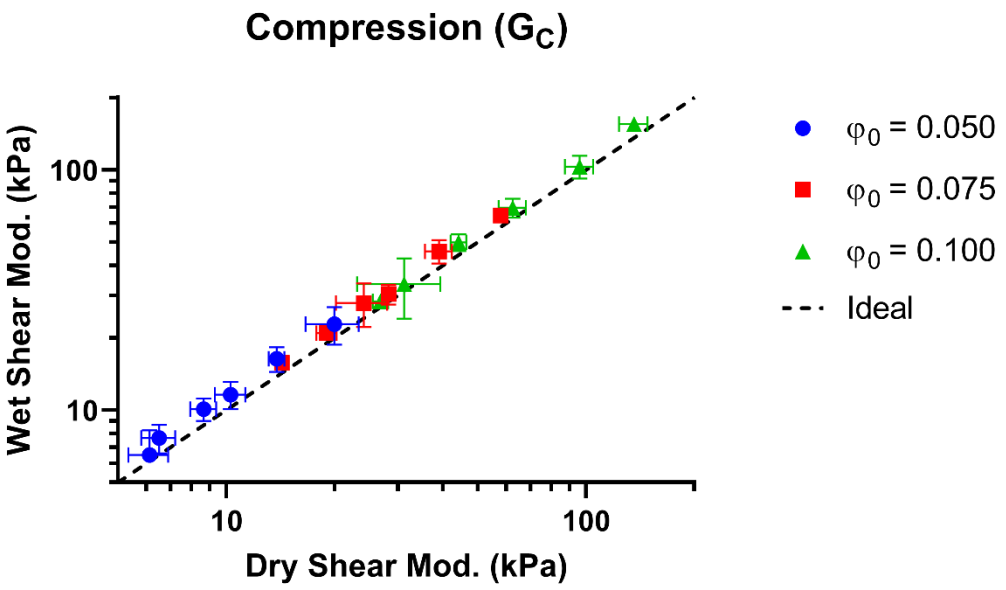

Supplementary Figure S2. Measured shear modulus with compression experiments in wet (PBS-submerged) and dry (exposed to air) conditions.

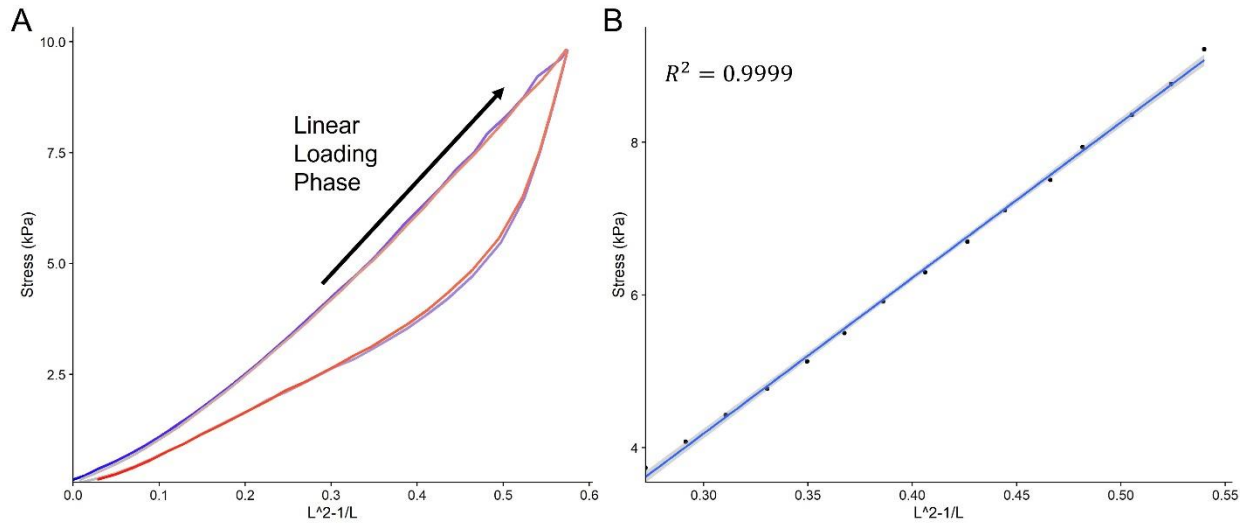

Supplementary Figure S3. Two loading and unloading cycles for each compression experiment yielded hysteresis but negligible plastic deformation (A). Shear modulus values were calculated from the upper half of the first loading phase for all experiments. Linear fit is shown in (B). Example curves were taken from the third compression sample for the $\varphi_0 = 0.050, N_j = 20$ formulation (Compression Exp. ID S1-PVA-M-50-400-3).

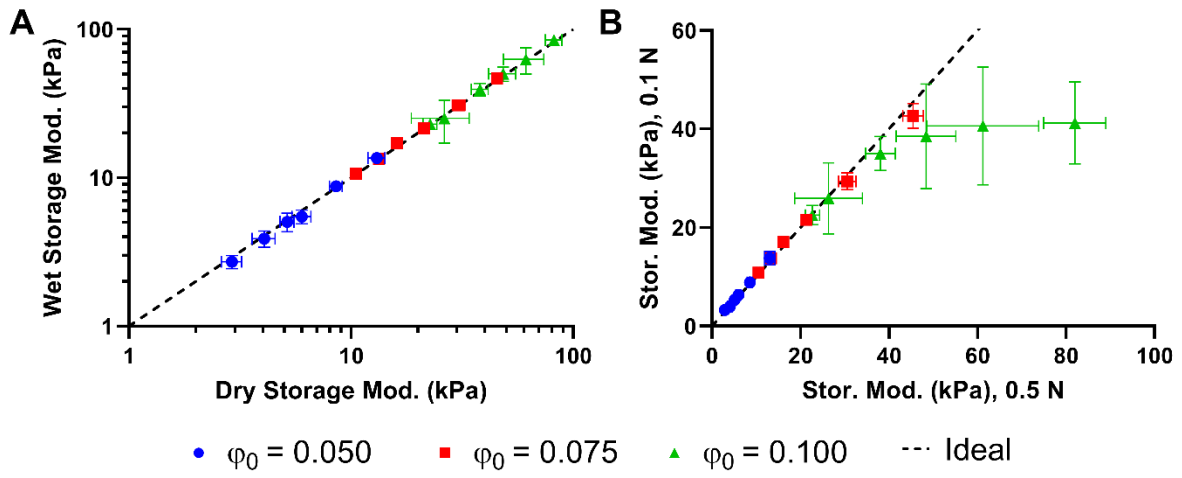

Supplementary Figure S4. Wet (PBS-submerged) and dry measurement conditions for rheological experiments on eighteen PVA hydrogel formulations (A) and measurements at two different axial forces (0.5 N vs. 0.1 N; B). In (A), all measurements were taken at 0.5 N axial force.

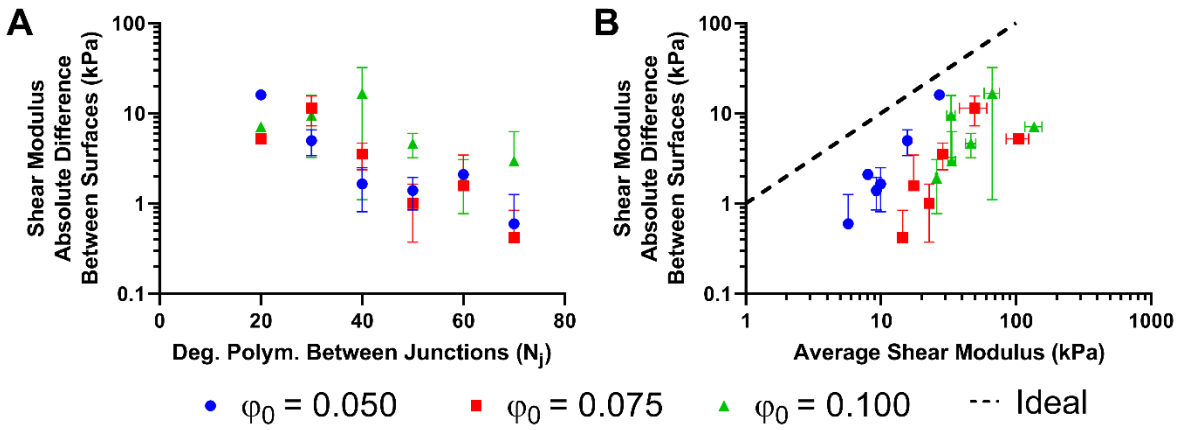

Supplementary Figure S5. Absolute differences between stiffnesses on opposite surfaces of hydrogel samples using nanoindentation. Decreasing degree of polymerization between junctions N_j (A) and increasing stiffness (B) loosely correlate to increased differences. Initial polymer volume fraction (φ_0) had no consistent effect.

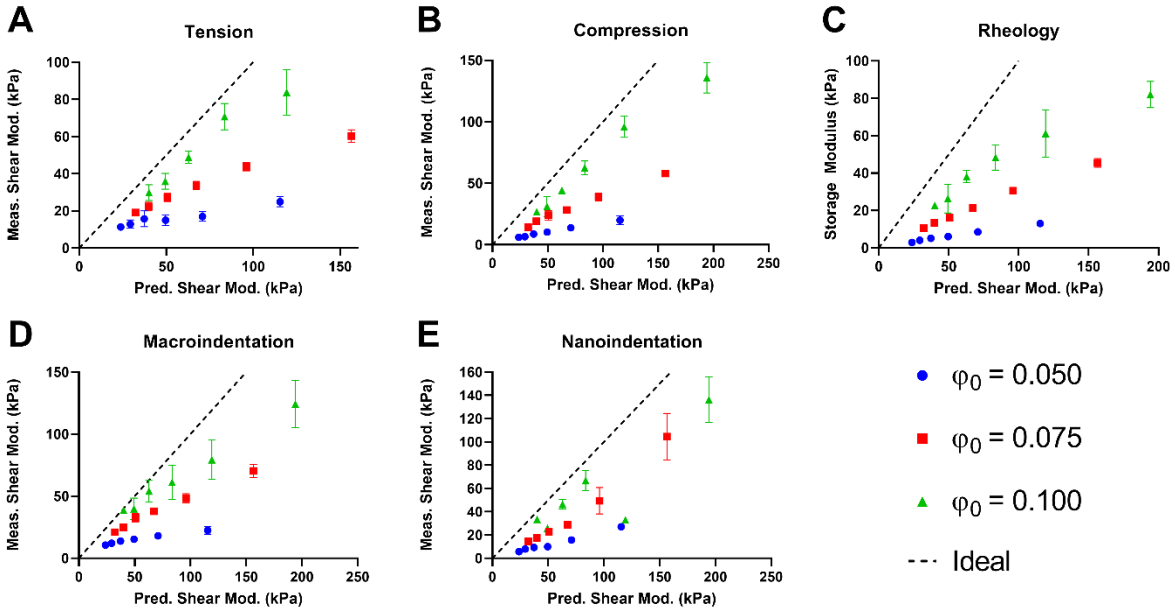

Supplementary Figure S6. Direct comparisons of measured and predicted stiffness values show that the predictions consistently overestimate measured values. They also show that the deviances are more significant at lower initial polymer volume fractions (φ_0) and lower degrees of polymerization between junctions (N_j, associated with higher stiffnesses within each φ_0 group).

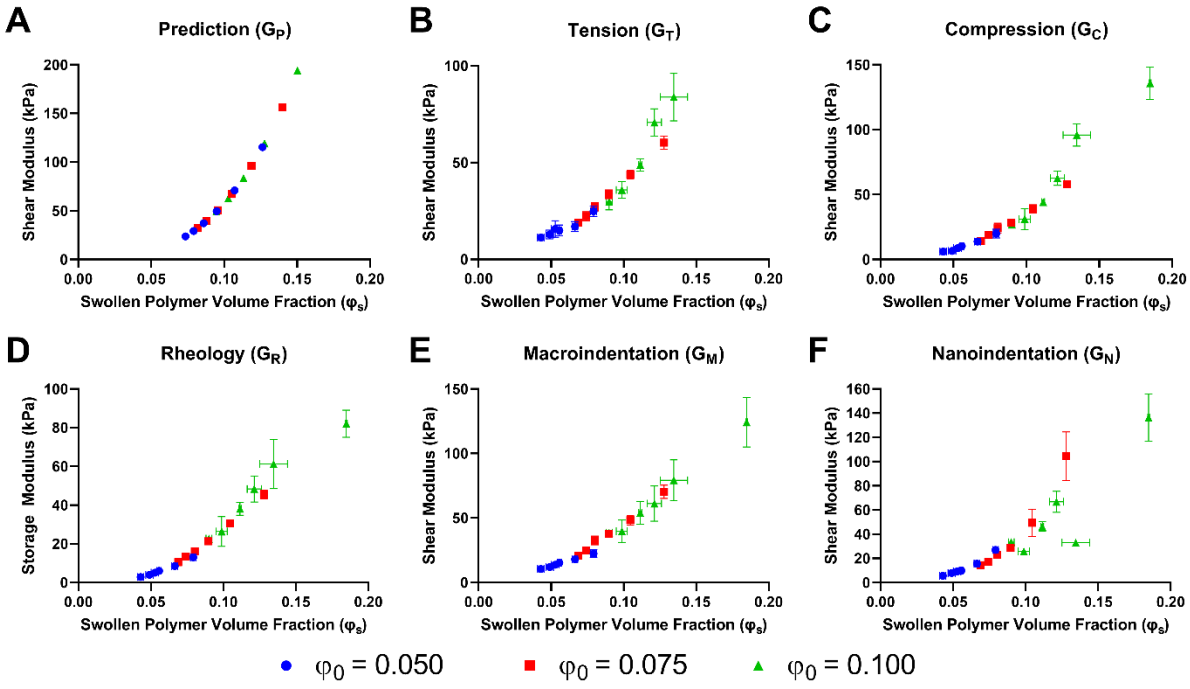

Supplementary Figure S7. Relationship between swelling and stiffness for each method. In (A), the predicted swollen polymer volume fraction (φ_s) is compared to the predicted shear modulus.

In (B-F), the measured swollen polymer volume fraction is compared to the measured shear modulus or storage modulus.

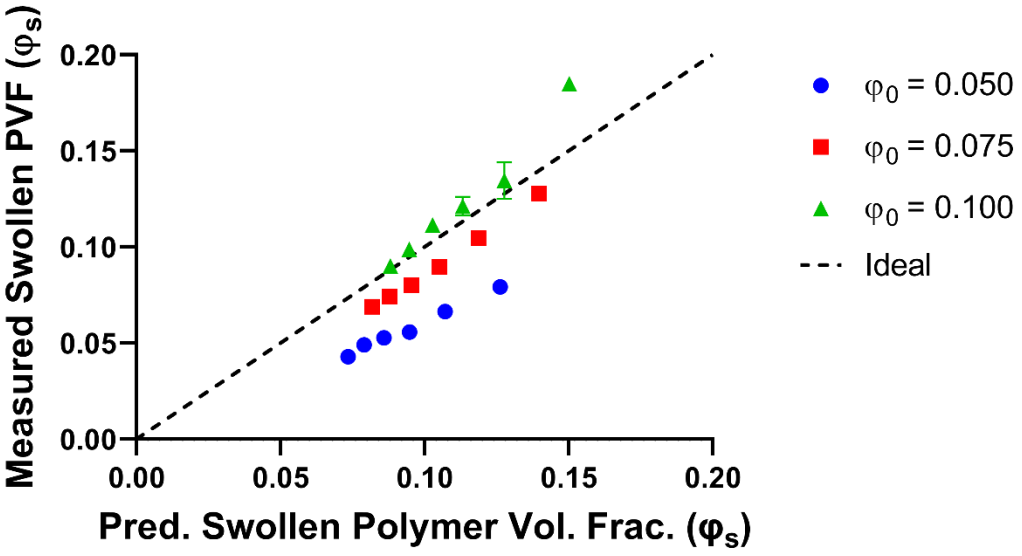

Supplementary Figure S8. Predicted and measured swollen polymer volume fraction of PVA hydrogels.